

Virtual VNA 2.0: *Ambiguity-Free* Scattering Matrix Estimation by Terminating Inaccessible Ports With *Tunable and Coupled* Loads

Philipp del Hougne, *Member, IEEE*

Abstract—We recently introduced the “Virtual VNA” concept which estimates the $N \times N$ scattering matrix characterizing an *arbitrarily complex* linear system with N monomodal ports by inputting and outputting waves only via $N_A < N$ ports while terminating the $N_S = N - N_A$ remaining ports with known tunable individual loads. However, vexing ambiguities about the signs of the off-diagonal scattering coefficients involving the N_S not-directly-accessible (NDA) ports remained. If only phase-insensitive measurements were used, an additional blockwise phase ambiguity ensued. Here, inspired by the emergence of “beyond-diagonal reconfigurable intelligent surfaces” in wireless communications, we lift all ambiguities with at most N_S additional measurements involving a known multi-port load network. We experimentally validate our approach based on an 8-port chaotic cavity, using a simple coaxial cable as two-port load network. Endowed with the multi-port load network, the “Virtual VNA 2.0” is now able to estimate the entire scattering matrix without any ambiguity, even without ever measuring phase information explicitly. Potential applications include the characterization of antenna arrays.

Index Terms—Virtual VNA, tunable load, impedance matrix estimation, scattering matrix, antenna array characterization, beyond-diagonal reconfigurable intelligent surface, phase retrieval, ambiguity, reverberation chamber.

I. INTRODUCTION

An *arbitrarily complex* linear passive time-invariant scattering system with N monomodal ports is fully characterized by its $N \times N$ scattering matrix. Traditionally, the latter is routinely and directly measured with an N -port vector network analyzer (VNA) for frequencies ranging from the radio-frequency via the microwave to the millimeter-wave regime. However, in important applications, it is desirable to be able to estimate the full scattering matrix without attaching a transmission line to each of the system’s ports: (i) the number of the system’s ports may drastically exceed the number of available VNA ports when characterizing large antenna arrays; (ii) some ports may be embedded (e.g., inside a circuit [1] or a biological system) and thus inaccessible; (iii) the attachment of a transmission line to the port may perturb the scattering properties of the system (e.g., a miniaturized antenna [2], [3]). We hence partition the system’s ports into accessible and

not-directly-accessible (NDA) ports. While no transmission line can be attached to an NDA port, it may nonetheless be possible to terminate the NDA port with a tunable load impedance. Is it possible to conceive a “virtual VNA” that retrieves the system’s full scattering matrix by measuring the “measurable” scattering matrix at the N_A accessible ports for different terminations of the N_S NDA ports?

Related questions have been studied in metrology for decades under terms like “unterminating” [4] (only studied for $N_S = 1$) and “port reduction” [5]–[7]. Port-reduction methods chiefly differ from the problem we address in the present work in that ports change between being accessible or NDA over the course of the studied methods.¹ For $N_S = 1$, the literature contains multiple experimental works tackling (sometimes in special scenarios) parts of the problem we address, in contexts spanning metrology and antenna characterization [4], [7], [9]–[18]. Two works [19], [20] studied parts of the problem we address in special scenarios with $N_S = 2$.

Recently, Refs. [21], [22] tackled the question of interest raised in the first paragraph in its entirety, considering the generic case of an *arbitrarily complex* system in Ref. [21]. It turned out that the full scattering matrix can be retrieved *up to sign ambiguities on off-diagonal terms associated with NDA ports if the terminations of the NDA ports can be switched between at least three distinct known load impedances*. A single directly accessible port is sufficient [22] but at least two directly accessible ports reduce the upper bound on the number of required load configurations by $N_S(N_S - 1)/2$ [21]. On the one hand, there is a closed-form approach, developed and numerically validated for the particular case of $N_A = 1$ in Ref. [22] and developed for the general case of $N_A > 1$ and experimentally validated in Ref. [21]. The closed-form approaches require specific load configurations and thereby define an upper bound on the number of required load configurations. Using more directly accessible ports improves the robustness to measurement noise. On the other hand, there is a gradient-descent approach compatible with (potentially opportunistic) random load configurations, developed and experimentally validated in Ref. [21]. The gradient-descent approach is generally more robust to measurement noise because the number of load configurations changing between measurements can strongly exceed one or two (for large N_S). Moreover, the gradient-descent approach can recover

The author acknowledges funding from the IETR PEPS program (project “IMPEST”), the ANR France 2030 program (project ANR-22-PEFT-0005), the European Union’s European Regional Development Fund, and the French region of Brittany and Rennes Métropole through the contrats de plan État-Région program (projects “SOPHIE/STIC & Ondes” and “CyMoCoD”).

P. del Hougne is with Univ Rennes, CNRS, IETR - UMR 6164, F-35000 Rennes, France (e-mail: philipp.del-hougne@univ-rennes.fr).

¹For the same reason, related recent efforts [8] based on embedded element radiation patterns are different from the problem we address here.

the full scattering matrix purely based on intensity-only data, except for a blockwise phase ambiguity in addition to the aforementioned sign ambiguities. None of the approaches requires specific characteristics of the three loads nor that they are the same at each NDA port [21].

Both fundamentally and for technological applications, an important question hence remains: how can these vexing ambiguities be lifted? Direct transmission measurements from *only one* accessible port to all NDA ports lift the ambiguities [21] but are not allowed if the NDA ports are “truly NDA”. In special cases, one can use a priori knowledge, e.g., about the system’s characteristics near dc [5]–[7] or the system’s geometric details [22]. Our goal, however, is a generically valid approach that can be applied to arbitrarily complex systems without any a priori knowledge.

The pivotal ingredient for a generic ambiguity-free approach is a *multi-port* load network (MPLN). All aforementioned approaches limit themselves to terminating NDA ports with individual one-port loads. The importance of using an MPLN was already recognized in Ref. [23] although this work only solved parts of the problem of estimating the *full* scattering matrix without *any* ambiguities that we address. MPLNs also appear in other contexts such as a variation of the port-reduction method [24] in metrology and beyond-diagonal reconfigurable intelligent surfaces (BD-RIS) [25]–[27] in wireless communications.

Remark 1. *Eliminating ambiguities is not at all required in other contexts such as end-to-end channel estimation in RIS-parametrized radio environments [28] or optimal non-invasive focusing on perturbation-inducing target inside a complex medium [29].*

Here, we demonstrate theoretically and experimentally that a proper solution to the ambiguity problem (fully in line with the NDA requirement) consists in using at least one known MPLN in addition to the three known tunable individual loads. The MPLN has at least two ports and can simply be a coaxial cable. After performing one of the three procedures outlined in Ref. [21], the coaxial cable is successively connected to pairs of NDA ports as well as once to one NDA and one accessible port. The use of coupled loads lifts all ambiguities (even in the case of intensity-only measurements) and thereby crowns the “virtual VNA” concept which can now operate free of any ambiguity, and even without ever measuring phase information.

Organization: In Sec. II, we propose a procedure to remove the sign ambiguity in the case of complex-valued measurements using a two-port load network (2PLN) and validate it experimentally. In Sec. III, we extend the method to the case of intensity-only measurements and validate it experimentally. In Sec. IV, we briefly conclude.

II. SIGN AMBIGUITY REMOVAL

Considering the case of complex-valued measurements, and assuming that either the closed-form or gradient-descent-based method detailed in Ref. [21] has been performed (without the “optional” sign ambiguity removal mentioned in

Ref. [21] based on directly accessing the NDA ports), in the present section we exclusively discuss how to remove the sign ambiguity of such an estimate using additional measurements involving a 2PLN. We detail the procedure in terms of impedance parameters but an equivalent implementation in terms of scattering parameters exists, as shown in Sec. III.

A. Background on sign ambiguity

To clearly understand the origin of the sign ambiguities and to appreciate the importance of the 2PLN in lifting them, let us consider a generic M -port system characterized by its impedance matrix $\tilde{\mathbf{Z}} \in \mathbb{C}^{M \times M}$. Two ports are terminated by a 2PLN characterized by its impedance matrix

$$\tilde{\mathbf{Z}}^{2\text{PLN}} = \begin{bmatrix} a & b \\ c & d \end{bmatrix} \in \mathbb{C}^{2 \times 2}, \quad (1)$$

where $b = c$ if the 2PLN is reciprocal; $b = c = 0$ if the 2PLN is composed of two individual (i.e., uncoupled) loads. The 2PLN terminates the k th and l th ports of the the M -port system, and the set \mathcal{F} contains the port indices of the remaining $M - 2$ ports. Using the convenient partition

$$\tilde{\mathbf{Z}} = \begin{bmatrix} \tilde{\mathbf{Z}}_{\mathcal{F}\mathcal{F}} & \tilde{\mathbf{z}}_k & \tilde{\mathbf{z}}_l \\ \tilde{\mathbf{z}}_k^T & \check{\zeta}_k & \check{\kappa}_{kl} \\ \tilde{\mathbf{z}}_l^T & \check{\kappa}_{kl} & \check{\zeta}_l \end{bmatrix}, \quad (2)$$

the measurable impedance matrix $\hat{\mathbf{Z}} \in \mathbb{C}^{(M-2) \times (M-2)}$ is [21], [30]

$$\begin{aligned} \hat{\mathbf{Z}} &= \tilde{\mathbf{Z}}_{\mathcal{F}\mathcal{F}} - [\tilde{\mathbf{z}}_k \quad \tilde{\mathbf{z}}_l] \left(\begin{bmatrix} \check{\zeta}_k & \check{\kappa}_{kl} \\ \check{\kappa}_{kl} & \check{\zeta}_l \end{bmatrix} + \begin{bmatrix} a & b \\ c & d \end{bmatrix} \right)^{-1} \begin{bmatrix} \tilde{\mathbf{z}}_k^T \\ \tilde{\mathbf{z}}_l^T \end{bmatrix} \\ &= \tilde{\mathbf{Z}}_{\mathcal{F}\mathcal{F}} - [\tilde{\mathbf{z}}_k \quad \tilde{\mathbf{z}}_l] \left(\tilde{\chi} \begin{bmatrix} \check{\zeta}_l + d & -(\check{\kappa}_{kl} + b) \\ -(\check{\kappa}_{kl} + c) & \check{\zeta}_k + a \end{bmatrix} \right) \begin{bmatrix} \tilde{\mathbf{z}}_k^T \\ \tilde{\mathbf{z}}_l^T \end{bmatrix}, \end{aligned} \quad (3)$$

where

$$\tilde{\chi} = ((\check{\zeta}_k + a)(\check{\zeta}_l + d) - (\check{\kappa}_{kl} + b)(\check{\kappa}_{kl} + c))^{-1}. \quad (4)$$

Assuming that the 2PLN is reciprocal for simplicity, we can rewrite Eq. (3) as follows:

$$\begin{aligned} \hat{\mathbf{Z}} &= \tilde{\mathbf{Z}}_{\mathcal{F}\mathcal{F}} - \tilde{\chi} [(\check{\zeta}_l + d)\tilde{\mathbf{z}}_k\tilde{\mathbf{z}}_k^T + (\check{\zeta}_k + a)\tilde{\mathbf{z}}_l\tilde{\mathbf{z}}_l^T \\ &\quad - (\check{\kappa}_{kl} + b)(\tilde{\mathbf{z}}_k\tilde{\mathbf{z}}_l^T + \tilde{\mathbf{z}}_l\tilde{\mathbf{z}}_k^T)]. \end{aligned} \quad (5)$$

All entries of the estimates of the vectors $\tilde{\mathbf{z}}_k$ and $\tilde{\mathbf{z}}_l$ have the same sign ambiguity $\pm\beta_k$ and $\pm\beta_l$, respectively [21]. The terms in Eq. (5) involving $\tilde{\mathbf{z}}_k\tilde{\mathbf{z}}_k^T$ and $\tilde{\mathbf{z}}_l\tilde{\mathbf{z}}_l^T$ are inevitably insensitive to the sign of $\tilde{\mathbf{z}}_k$ (and thereby to $\pm\beta_k$) and the sign of $\tilde{\mathbf{z}}_l$ (and thereby to $\pm\beta_l$), respectively.

If $b = 0$, then the term $\check{\kappa}_{kl}(\tilde{\mathbf{z}}_k\tilde{\mathbf{z}}_l^T + \tilde{\mathbf{z}}_l\tilde{\mathbf{z}}_k^T)$ cannot help to lift the sign ambiguities $\pm\beta_k$ and $\pm\beta_l$ because $\check{\kappa}_{kl}$ is itself not known without ambiguity. Instead,

$$\pm\kappa_{kl} = \pm\beta_k \pm\beta_l. \quad (6)$$

Moreover, $\tilde{\chi}$ is insensitive to the sign of $\check{\kappa}_{kl}$ (and thereby to $\pm\kappa_{kl}$).

In contrast, if $b \neq 0$, the term $\tilde{\chi}$ is sensitive to $\pm\kappa_{kl}$; moreover, the magnitude of the term $(\check{\kappa}_{kl} + b)(\tilde{\mathbf{z}}_k\tilde{\mathbf{z}}_l^T + \tilde{\mathbf{z}}_l\tilde{\mathbf{z}}_k^T)$ is sensitive to $\pm\kappa_{kl}$. Hence, $b \neq 0$ allows us to determine $\pm\kappa_{kl}$ by

predicting $\hat{\mathbf{Z}}$ for the two possible values of $\pm_{\hat{\kappa}_{kl}}$ and retaining the value whose corresponding estimate of \mathbf{Z} is closer to the corresponding measurement thereof. Having determined $\pm_{\kappa_{kl}}$ imposes constraints on the possible combinations of values that $\pm_{\hat{\beta}_k}$ and $\pm_{\hat{\beta}_l}$ can take, as seen in Eq. 6, but is not enough to determine $\pm_{\hat{\beta}_k}$ and $\pm_{\hat{\beta}_l}$ unless one of them is known a priori.

B. Method to lift sign ambiguity

With this background, we can conceive the following procedure to lift all ambiguities in our original problem of estimating \mathbf{Z} for an N -port system with N_S NDA ports.

For the first additional measurement, we connect the m th accessible port and the i th NDA port to the 2PLN. We terminate all other NDA ports with arbitrary known individual loads. Since there is no sign ambiguity about the mutual impedances between the m th accessible port and the other accessible ports, and the measurable impedance matrix is insensitive to $\pm_{\beta_q} \forall q \neq i$, this setup allows us to determine \pm_{β_i} . Specifically, we predict the measurable impedance matrix for the two possible values of \pm_{β_i} and retain the one yielding the prediction that is closer to the corresponding measurement.

For the second additional measurement, we connect the i th and j th NDA ports to the 2PLN. We terminate all other NDA ports with arbitrary known individual loads. Since the measurable impedance matrix is insensitive to $\pm_{\beta_q} \forall q \notin \{i, j\}$ and we know \pm_{β_i} from the previous step, this setup allows us to determine \pm_{β_j} . Specifically, we predict the measurable impedance matrix for the two possible values of \pm_{β_j} and retain the one yielding the prediction that is closer to the corresponding measurement.

For the remaining $N_S - 2$ additional measurements, we proceed similarly. We connect the 2PLN to one NDA port whose sign ambiguity we have previously lifted and one whose sign ambiguity is yet to be determined.

Remark 2. *The proposed method requires $N_A \geq 2$ because in the first step one accessible port is connected to the 2PLN and at least one accessible port must remain free for measurements.*

Remark 3. *Without the first additional measurement involving an accessible and an NDA port, we could only align all sign ambiguities such that $\pm_{\beta_1} = \pm_{\beta_2} = \pm_{\beta_i} = \dots$ but we could not know their value. Nonetheless, this would imply $\pm_{\kappa_{ij}} = 1 \forall \{i, j\}$ such that we would be able to determine \mathbf{Z}_{SS} free of ambiguities. Meanwhile, all entries of \mathbf{Z}_{AS} would be subject to the same sign ambiguity. Such a result may be sufficient in applications where only the block SS is of interest. Then, $N_A = 1$ is sufficient.*

Remark 4. *The gradient-descent-based method from Ref. [21] should directly (without any additional steps) yield an estimate of \mathbf{Z} (or \mathbf{S}) only featuring the same sign ambiguity on all entries of \mathbf{Z}_{AS} (see Remark 3) if the tunable individual loads were replaced by a tunable multi-port load network (as envisioned for BD-RIS). However, calibrating a tunable N_S -port load network such that its $N_S \times N_S$ impedance matrix is*

known for each configuration might require an N_S -port VNA in which case it could be prohibitively costly for large N_S .

The proposed principled method is simple (it requires only a coaxial cable as 2PLN) and has an acceptable linear complexity scaling (it requires N_S additional measurements).

C. Experimental validation

For our experimental validation, we leverage a simple 50-cm coaxial cable as 2PLN, as seen in Fig. 1C; its measured scattering and impedance characteristics are displayed in the right column of Fig. 1D. Except for the 2PLN, we use the same experimental setup as in Ref. [21] (shown in Fig. 1A,B). We do not have any a priori knowledge about the geometry or other details of our system. All experimental results presented here are based on electronically switching the individual loads using the setup displayed Fig. 1B. As seen in the left column of Fig. 1D, none of the three possible individual loads is close to an ideal open circuit or an ideal matched load at the considered frequencies between 740 MHz and 810 MHz. For the principled approach from Sec. III of Ref. [21], we hence do not have access to an ideal open circuit such that we must use the procedure from Sec. III-B in Ref. [21] that was not demonstrated experimentally so far. The additional measurements involving the 2PLN are realized by manually connecting the 2PLN to the required ports, as shown in Fig. 1C.

We quantify the accuracy of our estimated impedance or scattering matrix with a metric quantifying the ratio between signal and estimation error:

$$\zeta = \left\langle \frac{\text{SD} [Z_{ij}^{\text{GT}}(f)]}{\text{SD} [Z_{ij}^{\text{GT}}(f) - Z_{ij}^{\text{PRED}}(f)]} \right\rangle_{i,j,f}, \quad (7)$$

where SD denotes the standard deviation, and the superscripts GT and PRED denote ground truth and prediction, respectively. When we estimate scattering rather than impedance parameters, we replace Z_{ij} by S_{ij} in Eq. (7).

The experimentally achieved accuracies with the closed-form and gradient-descent approaches based on complex-valued measurements at the accessible ports are displayed in Fig. 2 as a function of the number of utilized measurements. In contrast to Ref. [21], we observe that the closed-form approach is very competitive in terms of achieved accuracy. We attribute this observation to two facts. On the one hand, the reproducibility of the electronic switching used here is much better than that of the manual switching used in Ref. [21] for the closed-form approach. The use of electronic switching implies that in general none of the three loads is an ideal open circuit, requiring the use of the method presented in Sec. III-B in Ref. [21] that we validate experimentally here for the first time. On the other hand, the results are obtained in the low-noise regime. The gradient-descent approach can be expected to become more advantageous as the level of noise increases because it can flexibly adapt the number of measurements and because the changes of the measurable scattering matrix are more significant (since more than one or two NDA port terminations are changed between any given pair of measurements) [21].

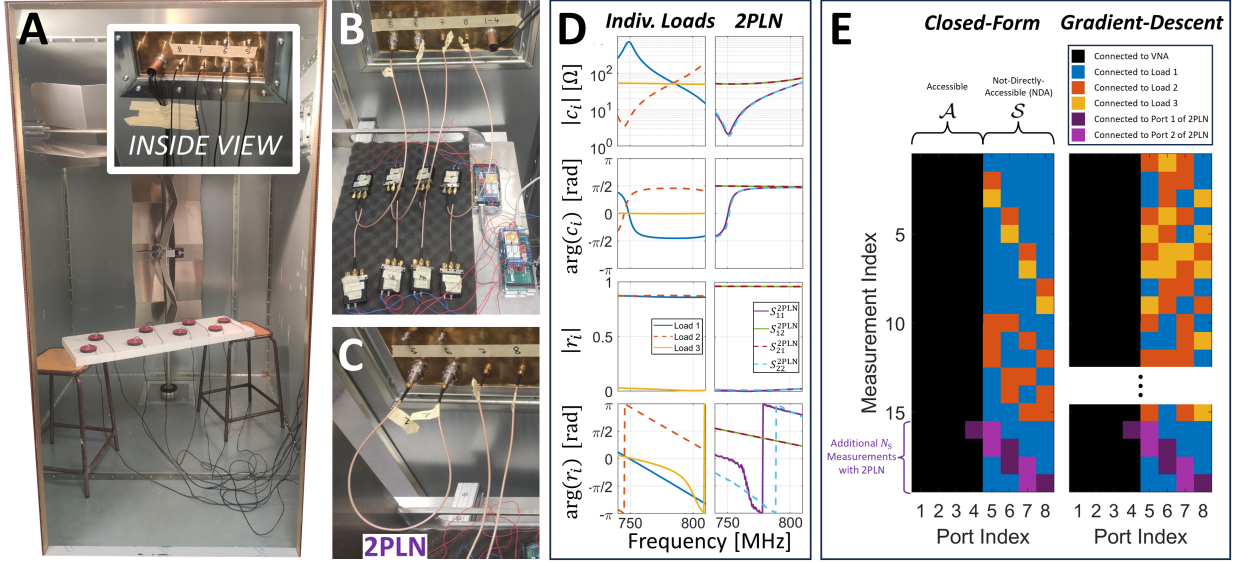


Fig. 1. Experimental setup. (A) Reverberation chamber comprising 8 antennas. (B) Setup to electronically switch the termination of four ports between three individual loads. (C) Setup involving the 2PLN (a coaxial cable). (D) Impedance and scattering characteristics of the three individual loads (left column) and the four coefficients characterizing the 2PLN (right column). (E) Measurement procedure for the “Virtual VNA 2.0”. \mathcal{A} and \mathcal{S} identify the accessible and NDA ports, respectively. The schematic shows whether a given port is connected to the VNA (black) or terminated by one of the three individual loads (blue, red, yellow) or the 2PLN (purple). The closed-form approach (left column) requires a series of specific configurations, the gradient-descent approach (right column) can be applied to an arbitrarily long sequence of random configurations (except for the last few involving the 2PLN).

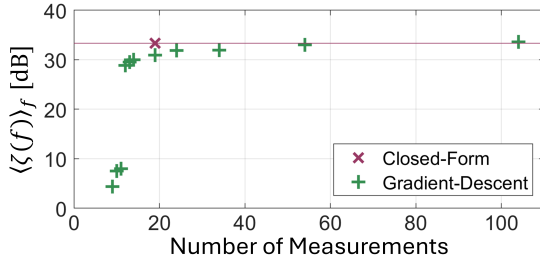


Fig. 2. Experimentally achieved frequency-averaged accuracy with complex-valued measurements.

Importantly, despite the lower reproducibility of manual switching in comparison to electronic switching, our reliance on manual switching for the N_S additional measurements involving the 2PLN did not pose a problem because these additional measurements are only used for binary sign decisions (as elaborated in Sec. II-B). Hence, the required accuracy for these additional measurements involving the 2PLN is lower than for the other measurements.

III. BLOCKWISE PHASE AMBIGUITY REMOVAL

In this section, we consider the case of phase-insensitive intensity-only measurements and work with scattering parameters, in line with the corresponding Sec. V in Ref. [21].

A. Background on phase ambiguity

Analogous to the developments in terms of impedance parameters in Sec. II-A, we first consider a generic M -port system terminated by a 2PLN. We can show using

$$\check{\mathbf{S}}^{2\text{PLN}} = \begin{bmatrix} e & f \\ g & h \end{bmatrix} \in \mathbb{C}^{2 \times 2}, \quad (8)$$

and the convenient partition

$$\check{\mathbf{S}} = \begin{bmatrix} \check{\mathbf{S}}_{\mathcal{F}\mathcal{F}} & \check{\mathbf{s}}_k & \check{\mathbf{s}}_l \\ \check{\mathbf{s}}_k^T & \check{\sigma}_k & \check{\nu}_{kl} \\ \check{\mathbf{s}}_l^T & \check{\nu}_{kl} & \check{\sigma}_l \end{bmatrix} \quad (9)$$

that (assuming the 2PLN is reciprocal, i.e., $f = g$)

$$\hat{\mathbf{S}} = \check{\mathbf{S}}_{\mathcal{F}\mathcal{F}} + \check{\xi} \left[(h - \check{\sigma}_l) \check{\mathbf{s}}_k \check{\mathbf{s}}_k^T + (e - \check{\sigma}_k) \check{\mathbf{s}}_l \check{\mathbf{s}}_l^T - (f - \check{\nu}_{kl}) (\check{\mathbf{s}}_k \check{\mathbf{s}}_l^T + \check{\mathbf{s}}_l \check{\mathbf{s}}_k^T) \right], \quad (10)$$

where

$$\check{\xi} = ((e - \check{\sigma}_k)(h - \check{\sigma}_l) - (f - \check{\nu}_{kl})^2)^{-1}. \quad (11)$$

Similarly to Sec. II-A, there is a sign ambiguity about $\check{\mathbf{s}}_k$ [$\check{\mathbf{s}}_l$] which we denote by $\pm \check{\gamma}_k$ [$\pm \check{\gamma}_l$] and about $\check{\nu}_{kl}$ which we denote by $\pm \check{\nu}_{kl}$. Furthermore, $\pm \check{\nu}_{kl} = \pm \check{\gamma}_k \pm \check{\gamma}_l$.

We now return to our original problem of determining \mathbf{S} for an N -port system with N_S NDA ports. A restriction to intensity-only measurements results in an additional blockwise phase ambiguity originating from the fact that the magnitudes of $e^{j\theta} \hat{\mathbf{S}}$ are insensitive to θ :

$$\left| \hat{\mathbf{S}} \right| = \left| e^{j\theta} \mathbf{S}_{\mathcal{A}\mathcal{A}} + \left(e^{j\theta/2} \mathbf{S}_{\mathcal{A}\mathcal{S}} \right) \left(\mathbf{S}_{\mathcal{L}}^{-1} - \mathbf{S}_{\mathcal{S}\mathcal{S}} \right)^{-1} \left(e^{j\theta/2} \mathbf{S}_{\mathcal{S}\mathcal{A}} \right) \right|, \quad \forall \theta. \quad (12)$$

Specifically, with individually tunable loads on the NDA ports, we can retrieve via gradient descent $e^{j\theta} \mathbf{S}_{\mathcal{A}\mathcal{A}}$ instead of $\mathbf{S}_{\mathcal{A}\mathcal{A}}$, $e^{j\theta/2} \mathbf{S}_{\mathcal{A}\mathcal{S}}^\pm$ (where \pm indicates column-wise sign ambiguities due to $\pm \check{\gamma}_i$) instead of $\mathbf{S}_{\mathcal{A}\mathcal{S}}$, and $\mathbf{S}_{\mathcal{S}\mathcal{S}}^\pm$ (where \pm indicates symmetric off-diagonal sign ambiguities due to $\pm \check{\nu}_{ij}$) instead of $\mathbf{S}_{\mathcal{S}\mathcal{S}}$, where θ is an unknown phase [21].

In sight of this blockwise phase ambiguity, let us reconsider the generic problem from the outset of this subsection

involving an M -port system terminated by a 2PLN for the specific case in which one of the two ports (the one indexed k) connected to the 2PLN is an accessible port and the other one (the one indexed l) is an NDA port. Due to the blockwise phase ambiguity, our estimate $\hat{\mathbf{S}}^{\text{PRED}}$ of \mathbf{S} obtained with intensity-only measurements is

$$\hat{\mathbf{S}}^{\text{PRED}} = \begin{bmatrix} e^{j\theta} \check{\mathbf{S}}_{\mathcal{F}\mathcal{F}} & e^{j\theta} \check{s}_k & e^{j\theta/2} \check{s}_l \\ e^{j\theta} \check{s}_k^T & e^{j\theta} \check{\sigma}_k & e^{j\theta/2} \check{\nu}_{kl} \\ e^{j\theta/2} \check{s}_l^T & e^{j\theta/2} \check{\nu}_{kl} & \check{\sigma}_l \end{bmatrix} \quad (13)$$

which implies

$$\xi^{\text{PRED}} = \left((e - e^{j\theta} \check{\sigma}_k)(h - \check{\sigma}_l) - (f - e^{j\theta/2} \check{\nu}_{kl})^2 \right)^{-1} \quad (14)$$

and

$$\hat{\mathbf{S}}^{\text{PRED}} = e^{j\theta} \left[\check{\mathbf{S}}_{\mathcal{F}\mathcal{F}} + \xi^{\text{PRED}} \left(e^{j\theta} (h - \check{\sigma}_l) \check{s}_k \check{s}_k^T + (e - e^{j\theta} \check{\sigma}_k) \check{s}_l \check{s}_l^T - e^{j\theta/2} (f - e^{j\theta/2} \check{\nu}_{kl}) (\check{s}_k \check{s}_l^T + \check{s}_l \check{s}_k^T) \right) \right]. \quad (15)$$

Various terms appearing in Eq. (14) and Eq. (15) are sensitive to the exact value of θ , such that in general $|\hat{\mathbf{S}}^{\text{PRED}}|$ equals $|\hat{\mathbf{S}}|$ only for $\theta = 0$.

B. Method to lift phase ambiguity

Using the same N_S additional measurement setups involving a 2PLN as in Sec. II but using intensity-only measurements here, we can lift both the sign and blockwise phase ambiguities. However, we proceed in the opposite order. First, we align all sign ambiguities such that all entries of \mathbf{S}_{AS} and \mathbf{S}_{SA} have the same sign ambiguity and that \mathbf{S}_{SS} is free of ambiguities. Then, we determine θ and fix the blockwise phase ambiguity that is specific to working with intensity-only data.

For the first additional measurement, we connect the first and second NDA ports to the 2PLN. We terminate the other NDA ports by arbitrary known individual loads. Then, we measure the intensities of the measurable scattering matrix. The predictions of the latter are insensitive to the value of θ as well as to $\pm\gamma_i \forall i > 2$. We predict the measurable scattering matrix intensities for the two possible values of $\pm\gamma_2$, and retain the one yielding the prediction that is closer to the corresponding measurement. Thereby, we impose $\pm\gamma_2 = \pm\gamma_1$.

For the next $N_S - 2$ measurements, we proceed similarly. We connect the 2PLN to one NDA port to which it has been connected previously and to one NDA port to which it has not been connected previously, in order to decide whether to flip the sign of the column and row corresponding to the latter.

Finally, we connect the 2PLN to the m th accessible port and the first NDA port. We terminate the remaining NDA ports with known arbitrary individual loads and measure the intensities of the measurable scattering matrix. We sweep the predictions of the latter through all possible values of θ and retain the value of θ for which the difference between the intensities of measured and predicted scattering coefficients are simultaneously approaching zero for each scattering coefficient. We observed numerically that examining

a single scattering coefficient may yield various possible values of θ ; therefore, it is important to ensure $N_A > 3$ in the case of intensity-only measurements such that the measurable scattering matrix is at least of dimensions 2×2 in the last measurement, providing three distinct scattering coefficients.

C. Experimental validation

Our experimental validation is based on the same setup as Sec. II-C but we assume that we are restricted to phaseless measurements here. We follow the procedure based on the gradient-descent method for intensity-only measurements detailed in Ref. [21] except for an improved procedure that aligns the phase offsets (see Appendix F in Ref. [21]): we take the median of θ^B obtained for multiple (rather than only one) previously aligned realizations.

Results of the various steps of the procedure outlined in Sec. III-B are displayed in Fig. 3 for the 771 MHz frequency point. The combined sign and blockwise phase ambiguities after the first step are apparent, and the remaining blockwise phase ambiguity after the second step is apparent, too. The final outcome is free of ambiguities and reaches an accuracy of 32 dB.

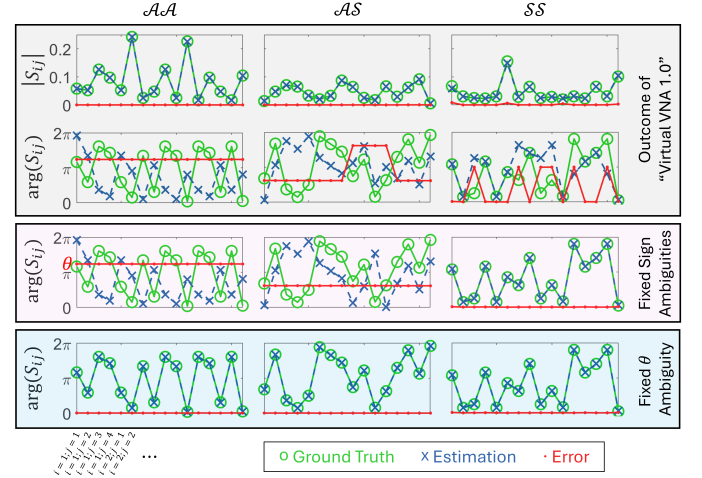


Fig. 3. Step-by-step procedure for ambiguity-free estimation of the full scattering matrix purely based on intensity-only measurements for 771 MHz. The resulting accuracy is $\zeta = 32$ dB.

Unlike the sign alignment, the estimation of θ to remove the blockwise phase ambiguity is not only a binary decision and hence significantly more vulnerable to reproducibility issues. Indeed, we encountered such issues at some frequency points. Future work will overcome these issues with a fully automated electronic switching setup, as shown in Fig. 4.

IV. CONCLUSION

We have theoretically and experimentally demonstrated the "Virtual VNA 2.0" which can estimate the full scattering matrix of an arbitrarily complex and unknown system without ever connecting a subset of N_S system ports to the VNA. The previously proposed Virtual VNA [21] solely used individual tunable loads to terminate the NDA ports such that it

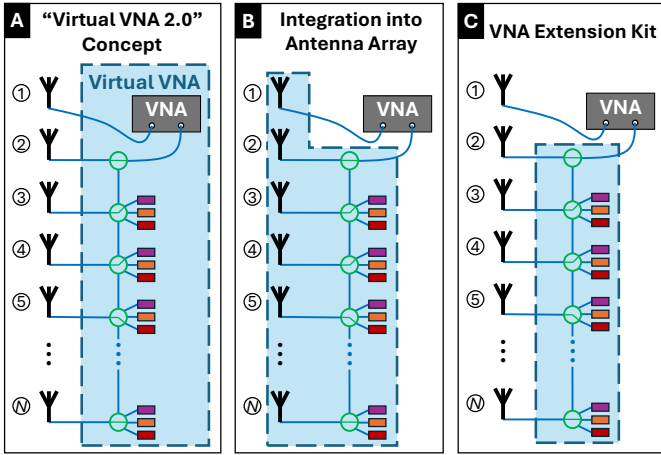


Fig. 4. Schematic of the setup of the proposed ambiguity-free “Virtual VNA 2.0” for the characterization of an N -element antenna array using a 2-port VNA. (A) Concept. (B) Implementation via integration into antenna array. (C) Implementation via VNA extension kit.

could not remove vexing sign ambiguities, and additional block-wise phase ambiguities in the case of phase-insensitive measurements. Here, we worked out and experimentally validated that MPLNs are the key to lifting these ambiguities. We found a very simple implementation, requiring only N_S additional measurements with a simple coaxial cable acting as 2PLN (i.e., the additional measurement complexity scales linearly with N_S).

Looking forward, we envision that the “Virtual VNA 2.0” approach presented here becomes an integral part of large-antenna-array characterization methods using a few-port VNA, as illustrated in Fig. 4A. The required tunable terminations of the antenna ports can be directly integrated into the antenna array itself (Fig. 4B) or they can be implemented in the form of a VNA extension kit (Fig. 4C). Importantly, the number of required switches scales linearly with N_S , in contrast to existing commercially available full-crossbar switch matrix solutions.

REFERENCES

- [1] Y. Zhang and J. Mao, “An overview of the development of antenna-in-package technology for highly integrated wireless devices,” *Proc. IEEE*, vol. 107, no. 11, pp. 2265–2280, 2019.
- [2] C. Icheln, J. Ollikainen, and P. Vainikainen, “Reducing the influence of feed cables on small antenna measurements,” *Electron. Lett.*, vol. 35, no. 15, pp. 1212–1214, 1999.
- [3] A. K. Skrivervik, J.-F. Zurcher, O. Staub, and J. Mosig, “PCS antenna design: The challenge of miniaturization,” *IEEE Antennas Propag. Mag.*, vol. 43, no. 4, pp. 12–27, 2001.
- [4] R. F. Bauer and P. Penfield, “De-embedding and unterminating,” *IEEE Trans. Microw. Theory Techn.*, vol. 22, no. 3, pp. 282–288, 1974.
- [5] H.-C. Lu and T.-H. Chu, “Port reduction methods for scattering matrix measurement of an n -port network,” *IEEE Trans. Microw. Theory Techn.*, vol. 48, no. 6, pp. 959–968, 2000.
- [6] —, “Multiport scattering matrix measurement using a reduced-port network analyzer,” *IEEE Trans. Microw. Theory Techn.*, vol. 51, no. 5, pp. 1525–1533, 2003.
- [7] U. R. Pfeiffer and C. Schuster, “A recursive un-termination method for nondestructive in situ S-parameter measurement of hermetically encapsulated packages,” *IEEE Trans. Microw. Theory Techn.*, vol. 53, no. 6, pp. 1845–1855, 2005.

- [8] D. Buck, K. F. Warnick, R. Maaskant, D. B. Davidson, and D. F. Kelley, “Measuring array mutual impedances using embedded element patterns,” *IEEE Trans. Antennas Propag.*, vol. 71, no. 1, pp. 606–611, 2022.
- [9] R. Garbacz, “Determination of antenna parameters by scattering cross-section measurements,” *Proc. Inst. Electr. Eng.*, vol. 111, no. 10, pp. 1679–1686, 1964.
- [10] J. T. Mayhan, A. R. Dion, and A. J. Simmons, “A technique for measuring antenna drive port impedance using backscatter data,” *IEEE Trans. Antennas Propag.*, vol. 42, no. 4, pp. 526–533, 1994.
- [11] M. Davidovitz, “Reconstruction of the S-matrix for a 3-port using measurements at only two ports,” *IEEE Microw. Guid. Wave Lett.*, vol. 5, no. 10, pp. 349–350, 1995.
- [12] U. Pfeiffer and B. Welch, “Equivalent circuit model extraction of flip-chip ball interconnects based on direct probing techniques,” *IEEE Microw. Wirel. Compon. Lett.*, vol. 15, no. 9, pp. 594–596, 2005.
- [13] U. R. Pfeiffer and A. Chandrasekhar, “Characterization of flip-chip interconnects up to millimeter-wave frequencies based on a nondestructive in situ approach,” *IEEE Trans. Adv. Packag.*, vol. 28, no. 2, pp. 160–167, 2005.
- [14] P. Pursula, D. Sandstrom, and K. Jaakkola, “Backscattering-based measurement of reactive antenna input impedance,” *IEEE Trans. Antennas Propag.*, vol. 56, no. 2, pp. 469–474, 2008.
- [15] S. Bories, M. Hachemi, K. H. Khelifa, and C. Delaveaud, “Small antennas impedance and gain characterization using backscattering measurements,” *Proc. EuCAP*, 2010.
- [16] A. J. Van Den Biggelaar, E. Galesloot, A. C. Franciscus, A. B. Smolders, and U. Johannsen, “Verification of a contactless characterization method for millimeter-wave integrated antennas,” *IEEE Trans. Antennas Propag.*, vol. 68, no. 5, pp. 3358–3365, 2020.
- [17] S. Sahin, N. K. Nahar, and K. Sertel, “Noncontact characterization of antenna parameters in mmw and thz bands,” *IEEE Trans. Terahertz Sci. Technol.*, vol. 12, no. 1, pp. 42–52, 2021.
- [18] D. Kruglov, P. Krasov, O. Iupikov, A. Vilenskiy, M. Ivashina, and R. Maaskant, “Contactless measurement of a D-band on-chip antenna using an integrated reflective load switch,” *IEEE Antennas Wirel. Propag. Lett.*, 2023.
- [19] W. Wiesbeck and E. Heidrich, “Wide-band multiport antenna characterization by polarimetric RCS measurements,” *IEEE Trans. Antennas Propag.*, vol. 46, no. 3, pp. 341–350, 1998.
- [20] B. Monsalve, S. Blanch, and J. Romeu, “Multiport small integrated antenna impedance matrix measurement by backscattering modulation,” *IEEE Trans. Antennas Propag.*, vol. 61, no. 4, pp. 2034–2042, 2013.
- [21] P. del Hougne, “Virtual VNA: Minimal-ambiguity scattering matrix estimation with load-tunable ports,” *arXiv:2403.08074*, 2024.
- [22] I. Shilinkov and R. Maaskant, “Antenna array measurements by a scalable backscatter modulation procedure,” *IEEE Antennas Wirel. Propag. Lett.*, pp. 1–5, 2024.
- [23] E. Denicke, M. Henning, H. Rabe, and B. Geck, “The application of multiport theory for MIMO RFID backscatter channel measurements,” in *Proc. EuMC*. IEEE, 2012, pp. 522–525.
- [24] Y.-C. Lin and T.-H. Chu, “Multiport scattering matrix determination from one-port measurements,” *IEEE Trans. Microw. Theory Techn.*, vol. 63, no. 7, pp. 2343–2352, 2015.
- [25] S. Shen, B. Clerckx, and R. Murch, “Modeling and architecture design of reconfigurable intelligent surfaces using scattering parameter network analysis,” *IEEE Trans. Wirel. Commun.*, vol. 21, no. 2, pp. 1229–1243, 2021.
- [26] H. Li, S. Shen, M. Nerini, M. Di Renzo, and B. Clerckx, “Beyond diagonal reconfigurable intelligent surfaces with mutual coupling: Modeling and optimization,” *IEEE Commun. Lett.*, vol. 28, no. 4, pp. 937–941, 2024.
- [27] P. del Hougne, “Physics-compliant diagonal representation of beyond-diagonal RIS,” *arXiv:2403.17222*, 2024.
- [28] J. Sol, H. Prod’homme, L. Le Magoarou, and P. del Hougne, “Experimentally realized physical-model-based frugal wave control in metasurface-programmable complex media,” *Nat. Commun.*, vol. 15, no. 1, p. 2841, 2024.
- [29] J. Sol, L. Le Magoarou, and P. del Hougne, “Optimal blind focusing on perturbation-inducing targets in sub-unitary complex media,” *arXiv:2401.15415*, 2024.
- [30] H. Prod’homme and P. del Hougne, “Efficient and updatable evaluation of arbitrarily complex connections between multi-port networks,” in *preparation*, 2024.